Secondary electron imaging of nonconductors with nanometer resolution

Milos Toth* and W. Ralph Knowles
FEI Company, 29 Water Street #216-217, Newburyport, Massachusetts 01950

Bradley L. Thiel
College of Nanoscale Science and Engineering, University at Albany at SUNY, 255 Fuller Rd, Albany, New York 12203

The resolution of secondary electron (SE) images in scanning electron microscopy (SEM) is limited by the SE diffusion length. However, most materials are poor electrical conductors and in practice, resolution and image information content are often limited by charging. We demonstrate how charging can be eliminated as the resolution-limiting factor using a gaseous SE detector for magnetic immersion electron lenses. Charging is stabilized by ions produced in a magnetic field-assisted gas ionization cascade. The charge control self-regulation process does not quench the SE imaging signal, thereby enabling high resolution image contrast mechanisms that are suppressed in high vacuum SEM.

Secondary electron (SE) image resolution in scanning electron microscopy (SEM) is on the order of a nanometer. It is determined by the diameter of the electron beam and the SE diffusion length. However, in practice, resolution and image contrast (i.e., information content) are often limited by charging. Charging gives rise to variations in the sample surface potential that can de-focus and deflect the beam during imaging, and cause recollection of electrons emitted from the specimen. It can be stabilized using a small amount of gas (~ 100 Pa) inside the specimen chamber.[1] This approach, termed low vacuum SEM (LVSEM), is well suited for high resolution imaging since the gas does not degrade image resolution provided the beam gas path length is shorter than the electron mean free path in the gas.[1] However, LVSEM has not previously been implemented on electron columns capable of producing maximum SEM resolution over a wide range of beam energy, referred to here as ultra-high resolution (UHR) columns, because of incompatibilities with the intense fields needed for UHR imaging. UHR columns utilize either a magnetic immersion lens, or an electrostatic retarding lens. The latter are incompatible with LVSEM because the intense electric field causes dielectric breakdown of the gas needed for charge control. The former use an intense magnetic field between the pole piece of the electron column and the sample surface. The magnetic field modifies the trajectories of secondary electrons emitted from the specimen, thereby preventing the use of conventional LVSEM detectors.

Here we demonstrate UHR imaging of nonconductors that charge severely in high vacuum SEM, using a low vacuum SE detector for magnetic immersion lens electron columns. The image resolution is not limited by charging. Charging is stabilized by ions produced in a gas ionization cascade that is used to amplify the SE signal. Images of insulators are shown to contain high resolution contrast that is absent in images obtained by high vacuum, low voltage SEM. These differences are interpreted in terms of the low vacuum charge control mechanism which does not rely on modulation of the SE yield, as is the case in low voltage, high vacuum SEM.

Figure 1 shows a cross-sectional schematic of the base of the pole piece of the electron column, and the LVSEM detector structure that was installed on a FEI Nova NanoSEM. The pressure limiting aperture (PLA) separates the high vacuum electron column from the low vacuum specimen chamber[1] (water vapor was the gas used inside the chamber). The detector electrodes are symmetric about the beam axis. The anode is biased (typically up to 400 V) and connected to an electrically floating pre-amplifier. The grounded "ion trap" electrode is used to enhance charge control. The detector and the sample are immersed in the magnetic field of the objective lens, which runs parallel to the beam axis. The field structure produced by the magnetic immersion lens and the biased anode causes secondary electrons to undergo axial oscillations along the beam axis, and cycloidal oscillations following the perimeter of the anode. Electrons undergoing the

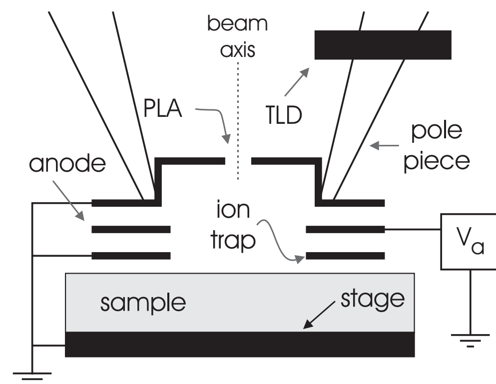

Figure 1. Cross-sectional schematic of the pole piece, electrodes making up the LVSEM detector, and the high vacuum thru-the-lens detector (TLD).

* e-mail: mtoth@FEICO.com

oscillatory motion collide with gas molecules and give rise to a gas ionization cascade that amplifies the SE signal, and generates gaseous ions used for charge control. Detailed analyses of electron trajectories, and the gas cascade process are presented elsewhere.[2]

Figure 2 shows high resolution images of: (a, b) a chrome-on-quartz photomask, (c) a contact hole in Si_3N_4, and (d) a pit in SiO_2 produced by an electrostatic discharge induced by a focused ion beam (in figure captions, P = gas pressure inside the specimen chamber and V_0 = electron beam accelerating voltage). The photomask consists of microscopic, electrically floating pieces of an optical absorber on a macroscopic, 6.25 mm tall quartz substrate. The absorber is identifiable by the grain structure clearly visible in both images. It consists of a 10 nm thick chrome oxide anti-reflective coating and a 90 nm chrome underlayer. In the high vacuum environments of conventional SEM and focused ion beam (FIB) tools, photomask imaging, metrology and repair are inhibited by severe charging.[3, 4] The low vacuum SE images in Figure 2 do not show charging artifacts. The resolution of the elevated magnification image in 2(b) is approximately 1 nm (it was measured by detecting all edges in the image, and calculating the average distance over which the imaging signal rises, across an edge, from 30% to 70% of the maximum intensity at each edge). The resolution is the same as in images of conductive gold-on-carbon resolution standards obtained by high vacuum SEM, demonstrating that it is limited by electron optical aberrations (i.e., beam diameter) rather than charging.

Images of the dielectrics shown in Figure 2(c) and (d) have a reduced resolution, in the range of 2-6 nm. These values probably correspond to the SE diffusion length, which places a fundamental limit on SE resolution. In insulators, the mean free paths (and hence the diffusion lengths) of low energy electrons are generally longer than in metals, due to the absence of electron-electron scattering at SE energies below the threshold for electron excitation across the bandgap.[5, 6] Hence, in insulators, SE diffusion is expected to limit resolution to an extent that is greater than in metals.[7] Exact effects on images will depend on the contrast mechanism (e.g., variations in the SE generation rate or the height of the surface barrier) and feature proximity to other features in the image.

We now turn to the topic of charging. Stable, high resolution imaging of nonconductors requires a charge control mechanism that does not rely on modulation of the electron beam landing energy, or the SE emission current. In low vacuum SEM, charging is stabilized by ions generated in the gas cascade which is used to amplify the imaging signal.[1] To illustrate the nature of low vacuum charge control, Figure 3 shows SE images of a pit in SiO_2, obtained using: (a, b) the high vacuum thru-the-lens detector (TLD) and (c, d) the low vacuum detector shown in Figure 1. Images a and b were acquired using an accelerating voltage of 750 V, selected so as to minimize charging using the procedure described in Joy & Joy (1996)[8]. A number of features are marked on the images: (1) a defocused edge in the middle of a high vacuum image, and (2-3) SE contrast that is present in low vacuum images only. To interpret these features, we turn to models of charge balance in high and low vacuum SEM.

The principle of charge conservation yields Equation 1, which must be satisfied at all times[5]

$$I_b = (\eta + \delta) I_b + I_S + \frac{dq}{dt}. \qquad (1)$$

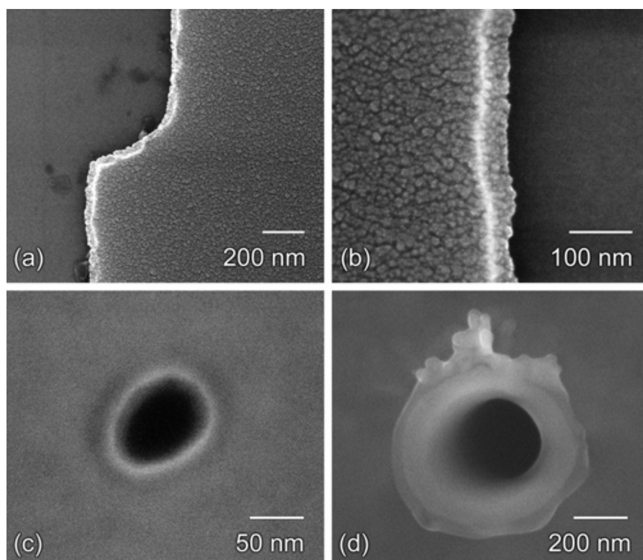

Figure 2. Low vacuum secondary electron images of: (a, b) chrome-on-quartz photolithographic mask [P = 100 Pa, V_0 = 17 kV], (c) contact hole in Si_3N_4 [P = 100 Pa, V_0 = 4 kV], (d) electrostatic discharge pit in SiO_2 [P = 40 Pa, V_0 = 7 kV].

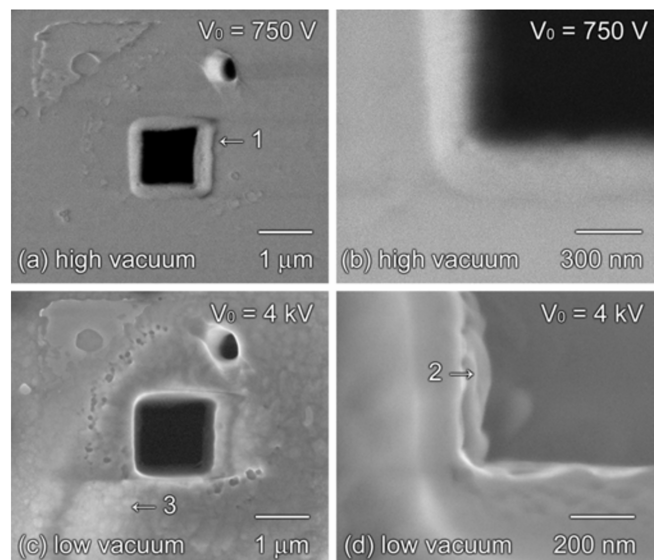

Figure 3. Secondary electron images of a pit in SiO_2 obtained by: (a, b) high vacuum, low voltage SEM, and (c, d) low vacuum SEM [P = 50 Pa]

I_b and I_s are the beam and specimen leakage current, η and δ are the backscattered and secondary electron yield, and dq/dt is the charge accumulation rate in the sample. In high vacuum SEM, dq/dt has a positively charged component corresponding to the holes left behind by SE emission, and a negative component corresponding to injected primary electrons[5]

$$\frac{dq^+}{dt} = -\delta I_b , \quad (2)$$

$$\frac{dq^-}{dt} = (1-\eta) I_b . \quad (3)$$

In the case of bulk insulators, $I_s \approx 0$. Hence, in the steady state (denoted by ∞), dq/dt must be zero, and (in high vacuum SEM)[5]

$$0 = (1-\eta_\infty - \delta_\infty) I_b , \quad (4)$$

$$\therefore \delta_\infty = 1 - \eta_\infty . \quad (5)$$

That is, in high vacuum SEM, steady state is attained by modulation of δ (since, at the low beam energies needed for high vacuum imaging of insulators,[8] the initial and steady state values of η are approximately equal: $\eta_\infty \approx \eta_{t=0}$). SE yield modulation occurs through two mechanisms:[5] (i) recollection of emitted secondaries by a net positive sample surface, and (ii) lowering of the electron beam landing energy by a net negative specimen surface. Both of these mechanisms give rise to imaging artifacts. The former lowers the SE imaging signal, and can quench image contrast, as is discussed below. The latter can generate electric fields that are sufficiently intense to defocus and deflect the electron beam. Low voltage SEM[8] aims to minimize such fields by setting the electron beam accelerating voltage so as to yield the steady state landing energy in the presence of a negligible surface potential. However, in general, the critical landing energy varies from point to point across the sample surface, thereby giving rise to artifacts such as feature 1 in Figure 3(a) (i.e., a defocused, distorted edge in the middle of an otherwise focused image).

Equation 5 implies that the steady state SE yield (δ_∞) is a function of η_∞ only. That is, all high resolution ("type 1")[7] SE contrast is generated during the transition from the initial to the steady state. The time constant associated with this transition is short relative to the pixel dwell times employed in SEM.[5] Hence, in high vacuum SEM images of insulators, the magnitude of the type 1 SE image component is low, and can not be increased by reducing the scan speed. This may explain the flat, featureless appearance of the high vacuum images shown in Figure 3(a) and (b) (relative to the corresponding low vacuum images c and d). Specifically, contrast within features 2 and 3 (indicated on Figure 3) is visible in low vacuum SE images only. The presence of such contrast in LVSEM images is discussed below.

In low vacuum SEM, positive gas ions neutralize (and hence generate holes) at the sample surface.[9] Hence, dq^+/dt has a component corresponding to the ion neutralization current (I_i)

$$\frac{dq^+}{dt} = -\delta I_b - I_i . \quad (6)$$

In the steady state (where $dq/dt = 0$) the sum of Equations 3 and 6 (i.e., the two components making up dq/dt) yields

$$\delta_\infty = (1-\eta_\infty) - \frac{I_{i\infty}}{I_b} . \quad (7)$$

This expression indicates that, in low vacuum SEM, the steady state can be attained by modulation of I_I instead of δ. Hence, high resolution, (type 1) SE contrast is clearly visible in low vacuum images of insulators, as is illustrated by features 2 and 3 marked on Figures 3(d-f). We note that this contrast does not correspond to sub-surface features located below the maximum penetration depth of the low energy (750 eV) electrons used to generate the images shown in Figures 3(a-b). The resolution of contrast generated by features below the SE escape depth is limited by beam spread below the sample surface. The resolution within features 2 and 3 is on the order of the SE escape depth in insulators, which is much shorter than the penetration depth of the high energy (4 keV) electrons used to take the LVSEM images shown in Figures 3d-f.

To achieve stable, artifact-free charge control, I_i must self-regulate as the beam is scanned across regions of samples exhibiting different charging behavior (e.g., the chrome-quartz interface or the pit shown in Figure 2(b) and 3(d), respectively). I_i can be made to self-regulate by making the fraction of ions reaching the specimen surface strongly dependent on the surface potential.[10, 11] This is achieved using the ion trap electrode shown in Figure 1, which acts as a sink of excess ions produced in the gas cascade (the high gas gains of $10^2 - 10^3$ provide a source of excess ions inside the detector volume[2]).

In conclusion, we demonstrated that magnetic immersion lens LVSEM can eliminate specimen charging as the resolution-limiting factor in secondary electron imaging. Low vacuum secondary electron images can contain high resolution contrast that is absent in high vacuum, low voltage SEM, due to differences between charge control self-regulation mechanisms in low and high vacuum SEM.

References

1. B.L. Thiel and M. Toth, *Secondary electron contrast in low-vacuum/environmental scanning electron microscopy of dielectrics.* J. Appl. Phys. **97**(5), 051101 (2005).
2. B.L. Thiel, M. Toth, R. Schroemges, H. Scholtz, G. van Veen and W.R. Knowles, *A Two-Stage Gas Amplifier for Ultra-High Resolution Low-*

Vacuum Scanning Electron Microscopy. Review of Scientific Instruments, in press (2006).
3. M.T. Postek and A.E. Vladar, *New application of variable-pressure/environmental microscopy to semiconductor inspection and metrology.* Scanning **26**(1), 11-17 (2004).
4. M.T. Postek, A.E. Vladar and M.H. Bennett, *Photomask dimensional metrology in the scanning electron microscope, part I: Has anything really changed.* J. Microlithogr. Microfabr. Microsyst. **3**(2), 212-223 (2004).
5. J. Cazaux, *Charging in scanning electron microscopy "from inside and outside".* Scanning **26**(4), 181-203 (2004).
6. A. Howie, *Threshold energy effects in secondary electron emission.* Microsc. microanal. **6**(4), 291-296 (2000).
7. H. Seiler, *Secondary-Electron Emission In The Scanning Electron-Microscope.* J. Appl. Phys. **54**(11), R1-R18 (1983).
8. D.C. Joy and C.S. Joy, *Low voltage scanning electron microscopy.* Micron **27**(3-4), 247-263 (1996).
9. M. Toth, M.R. Phillips, B.L. Thiel and A.M. Donald, *Electron imaging of dielectrics under simultaneous electron-ion irradiation.* J. Appl. Phys. **91**(7), 4479-4491 (2002).
10. J.P. Craven, F.S. Baker, B.L. Thiel and A.M. Donald, *Consequences of positive ions upon imaging in low vacuum scanning electron microscopy.* J. Microsc.-Oxf. **205**, 96-105 (2002).
11. M. Toth, M.R. Phillips, J.P. Craven, B.L. Thiel and A.M. Donald, *Electric fields produced by electron irradiation of insulators in a low vacuum environment.* J. Appl. Phys. **91**(7), 4492-4499 (2002).